



Title	Isolation and characterization of novel mutations in CDC50, the non-catalytic subunit of the Drs2p phospholipid flippase
Author(s)	Takahashi, Yasuhiro; Fujimura-Kamada, Konomi; Kondo, Satoshi et al.
Citation	The Journal of Biochemistry, 149(4), 423-432 https://doi.org/10.1093/jb/mvq155
Issue Date	2011-04
Doc URL	https://hdl.handle.net/2115/47953
Rights	This is a pre-copy-editing, author-produced PDF of an article accepted for publication in The Journal of Biochemistry following peer review. The definitive publisher-authenticated version J Biochem (2011) 149 (4): 423-432 is available online at: http://jb.oxfordjournals.org/content/149/4/423
Type	journal article
File Information	JoB149-4_423-432.pdf



Regular paper, Cell

Isolation and characterization of novel mutations in *CDC50*, the non-catalytic subunit of the Drs2p phospholipid flippase

Yasuhiro Takahashi^{1, 2, §}, Konomi Fujimura-Kamada^{1, 3, §}, Satoshi Kondo², and Kazuma Tanaka^{1, 3, *}

¹Division of Molecular Interaction, Institute for Genetic Medicine, Hokkaido University
Graduate Schools of Medicine² and Life Science³, N15 W7, Kita-ku, Sapporo, 060-0815,
Japan

Running title: Functions of Cdc50p in complex with Drs2p

Keywords: flippase, phospholipid asymmetry, type 4 p-type ATPase, yeast

*Kazuma Tanaka, Division of Molecular Interaction, Institute for Genetic Medicine, Hokkaido
University, N15 W7, Kita-ku, Sapporo, 060-0815, Japan. Phone: +81-11-706-5165, Fax:
+81-11-706-7821, E-mail address: k-tanaka@igm.hokudai.ac.jp

§These authors contributed equally to this work.

Abbreviations: CW, Calcofluor white; DIC, differential interference contrast; EGFP, enhanced green fluorescent protein; ER, endoplasmic reticulum; mRFP1, monomeric red fluorescent protein 1; PE, phosphatidylethanolamine; PC, phosphatidylcholine; PS, phosphatidylserine; TGN, *trans*-Golgi network; ts, temperature-sensitive.

Summary

Flippases (type 4 P-type ATPases) are believed to translocate phospholipids from the exoplasmic to the cytoplasmic leaflet in bilayer membranes. Since flippases are structurally similar to ion-transporting P-type ATPases such as the Ca^{2+} ATPase, one important question is how flippases have evolved to transport phospholipids instead of ions. We previously showed that a conserved membrane protein, Cdc50p, is required for the ER exit of the Drs2p flippase in yeast. However, Cdc50p is still associated with Drs2p after its transport to the endosomal/TGN membranes, and its function in the complex with Drs2p is unknown. In this study, we isolated novel temperature-sensitive (ts) *cdc50* mutants whose products were still localized to endosomal/TGN compartments at the non-permissive temperature. Mutant Cdc50 proteins colocalized with Drs2p in endosomal/TGN compartments, and they co-immunoprecipitated with Drs2p. These *cdc50-ts* mutants exhibited defects in vesicle transport from early endosomes to the TGN as the *cdc50* deletion mutant did. These results suggest that mutant Cdc50 proteins could be complexed with Drs2p, but the resulting Cdc50p-Drs2p complex is functionally defective at the non-permissive temperature. Cdc50p may play an important role for phospholipid translocation by Drs2p.

Introduction

In eukaryotic cells, plasma membrane phospholipids are asymmetrically distributed across the inner (cytosolic) and outer leaflets. The aminophospholipids phosphatidylserine (PS) and phosphatidylethanolamine (PE) are sequestered in the inner leaflet, whereas phosphatidylcholine

(PC) and sphingomyelin (SM) are enriched in the outer leaflet (1-3). The mechanism and physiological significance of establishing this asymmetrical distribution, however, are not thoroughly understood. The lipid asymmetry seems to be established and maintained by ATP-driven lipid transporters or translocases (1). One particular subfamily of the P-type ATPases, the P4 subfamily (P4-ATPase), has been implicated in aminophospholipid translocase (“flippase”) activities that move PS and PE from the outer to the inner leaflet (4) (for review). P4-ATPases are structurally similar to ion-transporting P type ATPases, but they transport phospholipids instead of ions. Thus, an important question is how P4-ATPases have evolved as flippases.

In the yeast *Saccharomyces cerevisiae*, the P4 subfamily contains five members, Drs2p, Dnf1p, Dnf2p, Dnf3p, and Neo1p (the Drs2/Dnf family). The quadruple deletion of the *DRS2* and all *DNF* genes results in lethality, although the individual single deletions are all viable, suggesting that *DRS2* and the *DNF* genes exert overlapping functions essential for cell growth (5). Drs2p and Dnf3p are localized to the endosomal/TGN system, whereas Dnf1p and Dnf2p are primarily localized to the plasma membrane (5-7). The *dnf1 dnf2* double deletion mutant exhibits a defect in the uptake of fluorescent 7-nitrobenz-2-oxa-1,3-diazol-4-yl (NBD)-labeled analogs of PE, PS, and PC across the plasma membrane (6). Natarajan *et al.* have demonstrated that Drs2p is involved in a flippase activity in TGN membranes (8), whereas Alder-Baerens *et al.* have shown that Drs2p and Dnf3p are responsible for a flippase activity in post-Golgi vesicles (9). More recently, PS-translocation activity has been detected in reconstituted proteoliposomes containing purified Drs2p (10) and in those containing purified mammalian retinal P4-ATPase Atp8a2 (11). These

studies strongly suggest that proteins in the P4 subfamily of P-type ATPases possess flippase activities.

Cdc50p, a conserved membrane protein identified as a factor required for polarized cell growth (12), and its two homologous proteins, Lem3p/Ros3p and Crf1p, constitute an essential family (the *CDC50* family) whose members have substantial functional overlap. Single deletions are viable, but the double deletion of *CDC50* and *LEM3* results in a severe growth defect, and the triple deletion of all *CDC50* family genes results in lethality (7, 13). Lem3p/Ros3p was first shown to be involved in the transport of NBD-labeled phospholipids across the plasma membrane (14, 15). We previously showed that the Cdc50p family forms a complex with members of the Drs2/Dnf family; Cdc50p, Lem3p and Crf1p form complexes with Drs2p, Dnf1p and Dnf2p, and Dnf3p, respectively (7, 16, 17). The formation of these complexes is essential for these proteins' exit from the ER and subsequent proper localization to the plasma membrane or endosomal/TGN membranes (7, 16, 17). This has also been shown to be the case in other organisms; a mammalian *CDC50* is required for the ER exit and transport of the *ATP8B1* flippase to the plasma membrane (18). In *Arabidopsis*, Cdc50 homolog ALIS proteins are required for the ER exit of P4-ATPases *ALA2* and *ALA3* (19, 20), and, in *Leishmania* parasites, LdRos3 is required for the ER exit of the LdMT flippase (21). These results suggest that the Cdc50 family proteins may function as chaperones for the P4-ATPases. However, Cdc50/Lem3 proteins still associate with P4-ATPases in the plasma membrane or endosomal/TGN membranes (7, 16), implying that they have functions other than chaperones when complexed with P4-ATPases. Since Cdc50 family proteins are unique

to P4-ATPases among P-type ATPases, they might have a function related to phospholipid flipping. Although recent biochemical results suggest that Cdc50p plays some role in the ATPase reaction cycle of Drs2p (22), *in vivo* evidence is still lacking. Identification of amino acid residues essential for its function as a subunit of P4-ATPase, not as a chaperone, would be informative to understand the molecular function of Cdc50 proteins.

In this study, we isolated novel temperature-sensitive (ts) mutations of *CDC50* whose products were properly localized to endosomal/TGN membranes but lost functions essential for cell growth in the absence of *LEM3* and *CRF1*. These mutant proteins were colocalized with Drs2p in endosomal/TGN compartments and were co-immunoprecipitated with Drs2p, but the mutants exhibited defects in the retrieval pathway from early endosomes to the TGN. These results could suggest that Cdc50p is required for the flippase function of Drs2p as a non-catalytic subunit.

Materials and Methods

Media and genetic techniques

Unless otherwise specified, strains were grown in YPDA rich medium (1% yeast extract [Difco Laboratories, Detroit, MI], 2% bacto-peptone [Difco], 2% glucose, and 0.01% adenine). Strains carrying plasmids were selected in synthetic medium (SD) containing the required nutritional supplements (23). In the screen for temperature-sensitive (ts) mutants, SD containing 0.1% 5-fluoroorotic acid (5-FOA; Wako Pure Chemicals, Osaka, Japan; SD + 5-FOA) was used to counterselect for the presence of *URA3*-containing plasmids. Calcofluor white (CW) sensitivity was tested on YPDA plates containing 100 µg/ml CW (Sigma-Aldrich, St. Louis, MO). Standard

genetic manipulations of yeast were performed as described (24). Yeast transformations were performed using the lithium acetate method (25, 26). *Escherichia coli* strains DH5 α and XL1-Blue were used for construction and amplification of plasmids.

Strains and plasmids

Yeast strains used in this study are listed in Table 1. Yeast strains carrying complete gene deletions (*cdc50* Δ , *crf1* Δ , *lem3* Δ , and *apl2* Δ), enhanced green fluorescent protein (EGFP)- or 13 x Myc-tagged *DRS2*, or monomeric red fluorescent protein 1 (mRFP1)-tagged *DRS2* and *SEC7* were constructed by polymerase chain reaction (PCR)-based procedures as described previously (27). The *chs6* disruption mutants on our strain background were constructed by introducing the PCR-amplified *chs6* Δ ::*kanMX4* allele (28). All constructs made by the PCR-based procedure were verified by colony-PCR amplification to confirm that replacement had occurred at the expected loci. *P(promoter)_{TRP1}-mRFP1-SNC1* strains were created by integrating the *EcoRV*-digested pKT1654 (pRS306-*P_{TRP1}*-mRFP1-SNC1) into the *URA3* locus followed by genetic crosses and dissection. The *CDC50-EGFP*, *cdc50-ts7-27-EGFP*, and *cdc50-ts9-4-EGFP* strains were constructed as follows. A linear DNA fragment containing *CDC50-EGFP-HIS3MX6*, *cdc50-ts7-27-EGFP-HIS3MX6*, or *cdc50-ts9-4-EGFP-HIS3MX6* gene, which is flanked with *CDC50*-promoter and –terminator sequences, was prepared by digestion of pKT1829, 1830, or 1831 with *KpnI* and *SalI*, respectively. This fragment was introduced into the strain YKT1697 (*cdc50* Δ ::*TRP1*) to replace *cdc50* Δ ::*TRP1* with the incoming *cdc50* allele and a His⁺ transformant

that exhibited tryptophan auxotrophy was selected.

Plasmids used in this study are listed in Table 2. Schemes detailing the construction of plasmids are available upon request.

Isolation of novel temperature-sensitive mutants of CDC50-EGFP

Temperature-sensitive *cdc50-EGFP* mutations, which caused lethality in combination with the *lem3Δ crf1Δ* mutations at 37°C but not at 25°C, were isolated by a PCR-based random mutagenesis technique (29). The mutagenic PCR was performed as described previously (30), using pKT1466 (pRS315-CDC50-EGFP) as a template and the oligonucleotides M13F (5'-TTGTAAAACGACGGCCAG-3') and M13R (5'-ACCATGATTACGCCAAGC-3'), which correspond to the sequences just outside the *CDC50-EGFP* gene on pKT1466, as primers. The purified mutagenized PCR products were mixed with an equal amount of pKT1466 without the *CDC50* gene prepared by digestion with *Bam*HI. This mixture of DNA was introduced into YKT1142 (*cdc50Δ lem3Δ crf1Δ* [YCplac33-CDC50]) to allow homologous recombination between the PCR products and the linearized plasmid, and the transformants were selected on SD-Leu at 25°C. The transformants were replicated on 5-fluoroorotic acid (5-FOA) plates and incubated at 25°C for 3 d to select against the original wild-type *CDC50* plasmid (YCplac33-CDC50 harboring *URA3*). Approximately 2.6×10^3 5-FOA-resistant colonies were tested for growth at 37°C on YPDA plates. From 8.8×10^3 initial transformants, 110 mutants that exhibited a temperature-sensitive (ts) growth defect were isolated. These 110 ts mutants were observed by

microscopy, and 39 *ts* mutants exhibited a normal endosomal/TGN localization pattern of Cdc50p-EGFP after incubation for 2 h at 37°C as well as at 25°C. From these mutants, plasmids were rescued and reintroduced into YKT1142 to confirm plasmid dependence of the phenotypes after loss of YCplac33-CDC50 (pKT1261). Six mutants exhibited a clear *ts* growth defect and a localization pattern of mutant Cdc50p-EGFP similar to that of wild-type Cdc50p-EGFP. We chose these mutants for further characterization.

Antibodies

Polyclonal anti-Cdc50p antibodies were prepared as follows: To create a plasmid for expression of Cdc50p fused to glutathione *S*-transferase (GST), the 570-bp DNA fragment coding for the carboxyl terminal 190 amino acids of Cdc50p was amplified by PCR and cloned into the *EcoRI-XhoI* sites of *E. coli* expression vector pGEX-4T-1 (Amersham Biosciences, Piscataway, NJ). The protein in the inclusion bodies was separated by SDS-PAGE and simultaneously stained with 0.0025% Coomassie Brilliant Blue G-250 (Wako Pure Chemicals) in SDS-PAGE Running buffer. The protein band was excised and eluted with elution buffer (100 mM Tris, pH6.8, 0.05% SDS). The eluted protein was used to immunize rabbits. Antiserum against Cdc50p was subsequently affinity-purified by passing the serum over a column of MBP-Cdc50p recombinant protein coupled to CNBr-activated Sepharose 4B (Amersham Biosciences). The MBP-Cdc50p expression plasmid was constructed by cloning the aforementioned *CDC50* DNA fragment into the *EcoRI-SalI* sites of *E. coli* expression vector pMAL-c2 (New England Biolabs, Beverly, MA). The protein was

purified by an amylose resin column (New England Biolabs) according to the manufacturer's instructions. The purified MBP-Cdc50p protein was covalently coupled to CNBr-activated Sepharose and incubated with antiserum for 2 h at 4°C. After washing out unbound antisera thoroughly, bound antibodies were eluted with 0.1 M glycine, pH 2.5. Eluates containing the affinity purified antibodies were immediately neutralized and stored at -80°C.

Mouse anti-Myc (9E10) monoclonal antibody was purchased from Sigma-Aldrich. The horseradish peroxidase (HRP)-conjugated secondary antibodies (sheep anti-mouse IgG and donkey anti-rabbit IgG) used for immunoblotting were purchased from Amersham Biosciences.

Immunoprecipitation and Western blotting

The preparation of crude membrane fractions was performed as described (7). Total membranes were solubilized in 0.8 ml of IP buffer (10 mM Tris-HCl, pH 7.5, 150 mM NaCl, 2 mM EDTA, 1% CHAPS) containing protease inhibitors (1 µg/ml aprotinin, 1 µg/ml leupeptin, 1 µg/ml pepstatin, 2 mM benzamide, 1 mM phenylmethylsulfonyl fluoride (PMSF)) and then centrifuged at 20,630 x g for 5 min at 4°C to remove insoluble materials. The cleared lysates were split into two aliquots; each was incubated with 5 µg of either anti-Myc antibody or control mouse IgG for 1 h at 4°C. These samples were rotated with 20 µl of protein-G Sepharose 4 Fast Flow (Pharmacia Biotech, Uppsala, Sweden) for 1 h at 4°C. The protein-G Sepharose beads were then pelleted and washed three times with IP buffer in the absence of detergents. The immunoprecipitates were separated by SDS-PAGE and transferred to polyvinylidene difluoride (PVDF) membranes. Western blotting

was performed as described previously (7). Protein bands were detected using LAS1000 mini luminescent image analyzer (Fuji Photo Film, Tokyo, Japan), and the signal intensity of the bands was quantified by Science Lab 2001 Image Gauge, version 4.0 (Fuji Photo Film).

Microscopic observations

Cells were observed using a Nikon ECLIPSE E800 microscope (Nikon Instec, Tokyo, Japan) equipped with a HB-10103AF super high-pressure mercury lamp and a 1.4NA 100 x Plan Apo oil immersion objective (Nikon Instec) with the appropriate fluorescence filter sets (Nikon Instec) and differential interference contrast (DIC) optics. Images were acquired with a digital cooled CCD camera (C4742-95-12NR; Hamamatsu Photonics K. K., Hamamatsu, Japan) using AQUACOSMOS software (Hamamatsu Photonics K. K.). To visualize EGFP- or mRFP1-tagged proteins, cells were grown to early-mid logarithmic phase, harvested, and resuspended in SD medium. Cells were mounted on microslide glass and observed using a GFP (green) bandpass filter set or G-2A (red) filter. Observations are based on the examination of at least 100 cells.

Results

Isolation of novel *cdc50* temperature-sensitive (*ts*) mutants

To investigate the functions of Cdc50p in complex with Drs2p, we attempted to isolate new temperature-sensitive *CDC50* mutant alleles, whose products are able to bind to Drs2p but are functionally defective. For this purpose, we took advantage of the retention of Cdc50p in the ER

when it does not bind to Drs2p (7); Cdc50p that can bind to Drs2p would be normally localized to endosomal/TGN compartments. To easily distinguish the localization of Cdc50p in mutants, we used the *CDC50-EGFP* allele in the screen. The *cdc50Δ* mutant is viable, but the *cdc50Δ lem3Δ crf1Δ* mutant is inviable, due to the combined defects in flippase activity of Drs2p, Dnf1/2p, and Dnf3p (7). The *cdc50Δ lem3Δ crf1Δ* cells harboring a plasmid containing randomly mutagenized *CDC50-EGFP* were tested for growth at 37°C. Mutants that exhibited a temperature-sensitive growth were re-examined for localization of Cdc50p-EGFP after a 2-h incubation at 37°C. Six temperature-sensitive mutants (*ts1-10*, *ts3-7*, *ts4-7*, *ts7-27*, *ts8-10*, and *ts9-4*), in which Cdc50p-EGFP resulted in a dotted fluorescence pattern characteristic of endosome/TGN-localized proteins, were selected (Fig. 1A and B). To confirm that these Cdc50p-ts proteins were actually localized to endosomal/TGN compartments, we examined the colocalization of Cdc50p-ts-EGFP with Sec7p-mRFP1, a TGN marker protein (31). Similar to wild-type cells, more than 70% of Cdc50p-ts-EGFP positive dots overlapped with Sec7p-mRFP1 dots after a 2-h incubation at 37°C in all *cdc50-ts* mutants, suggesting that Cdc50p-ts-EGFP mutant proteins normally localized to endosomal/TGN compartments (Fig. 1C).

We determined the mutation sites responsible for the temperature-sensitive growth defect. To define the region(s) containing such sites, we constructed chimeric genes consisting of the wild type- and mutant-derived regions by utilizing the *NheI* restriction enzyme site (Fig. 2A), and tested them for the growth phenotype. In four alleles, *cdc50-ts1-10*, *cdc50-ts3-7*, *cdc50-ts8-10*, and *cdc50-ts9-4*, the N-terminal region was responsible for the temperature sensitivity, whereas in

cdc50-ts4-7, the C-terminal region was responsible. In *cdc50-ts7-27*, both N- and C-terminal regions were necessary for the temperature-sensitive growth defect. DNA sequence analysis revealed that *cdc50-ts1-10*, *cdc50-ts8-10*, *cdc50-ts9-4*, and *cdc50-ts4-7* caused single amino-acid substitutions: I92T, F89S, Q71H, and P307S, respectively (Fig. 2A, rectangle). The other two mutations caused more than two amino acid substitutions; *cdc50-ts7-27* caused P23H and T320A, while *cdc50-ts3-7* caused L46P, I64N, N116S and E128K (Fig. 2A, rounded-rectangle).

To know whether the substituted amino acids are conserved in the Cdc50 family members from other organisms, the amino acid substitutions have been shown on the alignment of Cdc50p family proteins from yeast to human (Fig. 2B). Interestingly, four of the six mutant proteins contained substitutions in conserved residues. The proline 23 and the threonine 320 altered in *ts7-27* are conserved in the Cdc50 family, and, especially, the proline 23 is conserved in all Cdc50 family members. *ts4-7* also contained a substitution in the well-conserved proline residue at the 307 position. The glutamine 71 altered in *ts9-4* is conserved in fungal Cdc50 family members. Of three amino acids that are altered in *ts3-7*, leucine 46 is well conserved, whereas isoleucine 64 and asparagine 116 are less conserved. Interestingly, leucine 46 and isoleucine 64 are contained in the transmembrane region. These results suggest that the mutant Cdc50 proteins are defective in a conserved function in the Cdc50 family. As described below, further analysis of two of these *cdc50-ts* mutants (*ts7-27* and *ts9-4*) suggested that mutant proteins can interact with Drs2p, but are defective in the Drs2p functions: these substituted amino acids are implicated in proper functioning of Drs2p rather than interaction with Drs2p.

A *cdc50-ts* mutant whose Cdc50p product is immediately inactivated after the temperature shift would exhibit tight temperature-sensitivity for growth. The growth curve of the six temperature-sensitive mutants was examined after the temperature shift from 25°C to 37°C (Fig. 2C). Among these mutants, the *cdc50-ts7-27* and *cdc50-ts9-4* mutants exhibited the tightest temperature sensitivity. Thus, we used these two mutants for further phenotypic analyses.

Cdc50-ts mutant proteins can interact with Drs2p

If mutant Cdc50 proteins normally interact with Drs2p, they would be colocalized in endosomal/TGN compartments at a restrictive temperature. To observe the distribution of Cdc50-ts proteins and Drs2p in a single cell, we created *cdc50Δ lem3Δ crf1Δ DRS2-mRFP1* strains harboring the wild-type *CDC50-EGFP* or a *cdc50-ts-EGFP* plasmid. After a 2-h incubation at 37°C, almost all dotty signals of wild-type Cdc50p-EGFP overlapped with Drs2p-mRFP (Fig. 3A). Cdc50p-ts7-27-EGFP and Cdc50p-ts9-4-EGFP were also colocalized with Drs2p-mRFP, but some of them appeared as distorted structures rather than dotty structures. These shape changes of Cdc50p-Drs2p-positive structures seem to be due to defects in the endocytic recycling pathway (see below). In some cells of *cdc50-ts* mutants (~16% of *cdc50-ts7-27* and ~11% of *cdc50-ts9-4*), Drs2p-mRFP1 signals were observed in ER-like structures (Fig. 3A, an arrow). Thus, both mutant proteins are not fully functional in complex formation with Drs2p in the ER.

We next examined the interaction of Cdc50 mutant proteins with Drs2p by co-immunoprecipitation experiments. For this purpose, we constructed the *cdc50Δ lem3Δ crf1Δ*

DRS2-13Myc strain harboring the wild-type *CDC50-EGFP* or a *cdc50-ts-EGFP* plasmid. Cells were incubated for 2 h at 37°C before preparation of a crude membrane fraction. Drs2p-13Myc was immunoprecipitated from membrane protein extracts prepared by solubilization in 1% CHAPS. The resulting immunoprecipitates were analyzed by immunoblot with anti-Myc and -Cdc50p antibodies. Like wild-type Cdc50p-EGFP, both Cdc50p-ts7-27-EGFP and Cdc50p-ts9-4-EGFP were detected in immunoprecipitates from Drs2p-13Myc expressing cells, although the relative amount of Cdc50p-ts7-27-EGFP bound to Drs2p-13Myc was about half compared to wild-type Cdc50p-EGFP (Fig. 3B). Cdc50p-EGFP was not detected in either control immunoprecipitates with nonspecific IgG (data not shown) or those from cells lacking *DRS2-13Myc* (Fig. 3B). These data indicated that both Cdc50p-ts7-27-EGFP and Cdc50p-ts9-4-EGFP formed a complex with Drs2p at 37°C.

cdc50-ts mutants exhibit defects in membrane trafficking

Complex formation between mutant Cdc50 proteins and Drs2p at a restrictive temperature suggested that Cdc50p is required for the Drs2p function in the Cdc50p-Drs2p complex. For example, Cdc50p might be required for the flippase activity of Drs2p, and Cdc50-ts mutant proteins may be defective in this function. Since Cdc50p and Drs2p have been implicated in membrane trafficking from early endosome to the TGN, we examined *cdc50-ts* mutants for these phenotypes.

The chitin synthase III (Chs3p), which synthesizes cell wall chitin, is recycled through the early endosome and the TGN to the plasma membrane (32, 33). Wild-type cell growth is

sensitive to Calcofluor white (CW), a chitin-binding compound, whereas a mutant in the *CHS5* or *CHS6* coat complex is resistant, due to the retention of Chs3p in the TGN (34). It was previously shown that a mutant in the AP-1 clathrin adaptor complex restored the CW sensitivity in the *chs6Δ* mutant, possibly because the AP-1 mutation caused rerouting of Chs3p to the plasma membrane by inhibiting the early endosome-to-TGN transport of Chs3p. A *drs2Δ* mutation also exhibited this effect, suggesting that Drs2p is involved in the AP-1 function (35). We tested whether *cdc50-ts* mutations also conferred CW sensitivity on the *chs6Δ* mutant, and found that they did so in a temperature-dependent manner as *cdc50Δ* and *apl2Δ* (the β subunit of AP-1) mutations did (Fig. 4). These results suggest that *cdc50-ts7-27* and *cdc50-ts9-4* mutations impair the Drs2p function in the AP-1-mediated early endosome-to-TGN trafficking pathway.

We have recently shown that a conventional temperature-sensitive mutant in *CDC50* (*cdc50-ts lem3Δ crf1Δ*) exhibited an endocytic recycling defect and consequent mislocalization of Snc1p, an exocytic v-SNARE, to the early endosome (16). These results suggest that the flippase activity of Cdc50p-Drs2p is required for vesicle formation from early endosomes. If Cdc50-ts proteins impair the Drs2p function even when they are complexed with Drs2p, both Cdc50p-ts and Drs2p would be colocalized with Snc1p to endosomal membranes that are defective in vesicle formation. mRFP1-Snc1p was expressed in the *cdc50Δ lem3Δ crf1Δ* mutant containing the wild-type or mutant *cdc50-ts-EGFP* plasmid. These cells were cultured at 25°C, shifted to 37°C for 2 h, and examined microscopically. In wild-type *CDC50-EGFP* cells, mRFP-Snc1p was primarily localized to the bud (daughter cell) plasma membrane (98.6% of the cells, n=143), where

active exocytosis is occurring, and some population was localized to internal dotted structures that appeared to be early endosomes or TGN compartments (Fig. 5A) as previously reported (16, 36). In contrast, in cells harboring the *cdc50-ts7-27-EGFP* or *cdc50-ts9-4-EGFP* plasmid, significant population of the cells, 27.1% (n=133) or 33.3% (n=144), respectively, exhibited localization of mRFP1-Snc1p only to intracellular structures. These intracellular structures seem to be aberrant endosomal membranes that are defective in vesicle formation (16). Cdc50p-ts7-27-EGFP and Cdc50p-ts9-4-EGFP signals overlapped with these mRFP1-Snc1 membranes (Fig. 5A), suggesting that Cdc50-ts proteins are localized in accumulated endosomal membranes.

We next examined whether Drs2p was also localized to these mRFP1-Snc1p-containing endosomal membranes. We constructed the GFP-untagged version of *cdc50-ts7-27* and *cdc50-ts9-4*, and expressed *DRS2-EGFP* and *mRFP1-SNC1* in these *cdc50-ts lem3Δ crf1Δ* mutants. After a 2.5-h incubation at 37°C, 20.2% (n=173) and 15.1% (n=159) of *cdc50-ts7-27* and *cdc50-ts9-4* cells, respectively, exhibited localization of mRFP1-Snc1p only to intracellular membranes. Drs2p-EGFP signals, except for ER-like signals, also overlapped with these mRFP1-Snc1p structures (Fig. 5B). Taken together, these results suggest that the Cdc50-ts-Drs2p complexes are not able to promote vesicle formation from early endosomes at 37°C.

Discussion

Cdc50p seems to be stably associated with Drs2p in the endosomal/TGN compartments, but its function in the complex has remained unknown. Cdc50-ts proteins isolated in this study were

defective in the formation of transport vesicles from early endosomes to the TGN, even though they were associated with Drs2p in endosomal structures in which Snc1p seemed to be trapped. Thus, we propose that, in addition to its role as a chaperone for Drs2p in the ER exit, Cdc50p plays an important role for the flippase function of Drs2p in the endosomal/TGN compartments.

P4-ATPases transport lipids from the outer leaflet to the cytoplasmic leaflet, in the direction opposite to that of cation transport by other types of P-type ATPases. In addition, the size of a substrate phospholipid is much larger than that of metal ions. Structural conservation of core sequences in P4-ATPases raises an intriguing question: how have cation-transporting P-type ATPases evolved into these unique lipid-translocating P-type ATPases? Because the Cdc50 family is unique to P4-ATPases, possible functional involvement of Cdc50 in the flippase activity of P4-ATPases should be investigated. Complex formation with a transmembrane protein is an uncommon feature for P-type ATPases, but it is well known that the catalytic subunit of Na⁺, K⁺ ATPase is tightly associated with the noncatalytic β subunit, a single-pass transmembrane protein. The β subunit of Na⁺, K⁺ ATPase facilitates the correct membrane integration and packing of the catalytic α subunit, but in addition to this chaperone function, the β subunit is involved in the intrinsic transport properties of the mature Na⁺, K⁺ ATPases (37). Cdc50p is not homologous to this β subunit of Na⁺, K⁺ ATPase, but it may have evolved as an accessory protein specifically required for phospholipid flipping by the catalytic subunit.

Recently, a flippase activity has been reconstituted into proteoliposomes with affinity-purified Drs2p (10). In this reconstitution reaction, active Drs2p molecules were

estimated to be about 10% of total Drs2p molecules. Interestingly, since Drs2p was affinity-purified from yeast lysates, some Cdc50p was co-purified, and its molar concentration was found to be about 10% of Drs2p. Thus, the detected flippase activity may be ascribed to Cdc50p-Drs2p complexes. Another recent report suggests that Cdc50p plays a pivotal role for the ATPase reaction cycle of Drs2p (22). The ATPase reaction cycle of P-type ATPase has been intensively studied in the Ca²⁺ ATPase SERCA, and amino acid substitutions that block the reaction cycle at a specific point are known. They constructed analogous mutants in Drs2p, tested them for the interaction with Cdc50p, and found that the affinity of Drs2p for Cdc50p fluctuates during the reaction cycle, with the strongest interaction at a step where Drs2p is loaded with phospholipid ligand. They also showed that the complex formation with Cdc50p was required for the formation of phosphorylated intermediate of Drs2p, which is an essential step of the P-type ATPase reaction cycle.

The above results suggest that Cdc50p dynamically interacts with Drs2p during the reaction cycle of phospholipid flipping. As discussed in the above study (22), two transmembrane helices provided by Cdc50p may contribute to make the complex capable of flipping a phospholipid. Interestingly, amino acid substitutions found in Cdc50-ts proteins were close to or in either of two transmembrane regions. Of two mutants intensively characterized in this study, ts9-4 carried the Q71H substitution 8 amino acids downstream of the first transmembrane domain, and ts7-27 carried the P23H substitution 22 amino acids upstream of the first transmembrane domain and the T320A substitution 10 amino acids upstream of the second transmembrane domain.

Co-immunoprecipitation and quantitative analysis suggested that Cdc50p-ts7-27-EGFP exhibited a lower affinity to Drs2p, whereas Cdc50p-ts9-4-EGFP exhibited a normal affinity. The proline 23 or/and the threonine 320 may be crucial for Cdc50p to interact more strongly with Drs2p during the flippase reaction cycle. The glutamine 71 does not affect the interaction step, but may be involved in the promotion of the reaction cycle. The roles of these amino acids in the flippase reaction cycle need to be investigated by *in vitro* reconstitution assays in future studies.

Funding

This work was supported by Grants-in-Aid for Scientific Research from the Japan Society for the Promotion of Science and the Ministry of Education, Culture, Sports, Science and Technology of Japan to K. F.-Kamada and K. Tanaka.

Conflict of interest

None declared.

Acknowledgments

We thank Drs. Michael Lewis, Hugh Pelham, and Roger Tsien for plasmids. We thank our colleagues in the Tanaka laboratory for valuable discussions. We also thank Eriko Itoh for technical assistance.

References

1. Devaux, P.F. (1991) Static and dynamic lipid asymmetry in cell membranes. *Biochemistry* **30**, 1163-1173
2. Cerbon, J., and Calderon, V. (1991) Changes of the compositional asymmetry of phospholipids associated to the increment in the membrane surface potential. *Biochim. Biophys. Acta* **1067**, 139-144
3. Diaz, C., and Schroit, A.J. (1996) Role of translocases in the generation of phosphatidylserine asymmetry. *J. Membr. Biol.* **151**, 1-9
4. Paulusma, C.C., and Oude Elferink, R.P. (2005) The type 4 subfamily of P-type ATPases, putative aminophospholipid translocases with a role in human disease. *Biochim. Biophys. Acta* **1741**, 11-24
5. Hua, Z., Fatheddin, P., and Graham, T.R. (2002) An essential subfamily of Drs2p-related P-type ATPases is required for protein trafficking between Golgi complex and endosomal/vacuolar system. *Mol. Biol. Cell* **13**, 3162-3177
6. Pomorski, T., Lombardi, R., Riezman, H., Devaux, P.F., Van Meer, G., and Holthuis, J.C. (2003) Drs2p-related P-type ATPases Dnf1p and Dnf2p are required for phospholipid translocation across the yeast plasma membrane and serve a role in endocytosis. *Mol. Biol. Cell* **14**, 1240-1254
7. Saito, K., Fujimura-Kamada, K., Furuta, N., Kato, U., Umeda, M., and Tanaka, K. (2004) Cdc50p, a protein required for polarized growth, associates with the Drs2p P-Type ATPase

- implicated in phospholipid translocation in *Saccharomyces cerevisiae*. *Mol. Biol. Cell* **15**, 3418-3432
8. Natarajan, P., Wang, J., Hua, Z., and Graham, T.R. (2004) Drs2p-coupled aminophospholipid translocase activity in yeast Golgi membranes and relationship to *in vivo* function. *Proc. Natl. Acad. Sci. USA* **101**, 10614-10619
 9. Alder-Baerens, N., Lisman, Q., Luong, L., Pomorski, T., and Holthuis, J.C. (2006) Loss of P₄ ATPases Drs2p and Dnf3p disrupts aminophospholipid transport and asymmetry in yeast post-Golgi secretory vesicles. *Mol. Biol. Cell* **17**, 1632-1642
 10. Zhou, X., and Graham, T.R. (2009) Reconstitution of phospholipid translocase activity with purified Drs2p, a type-IV P-type ATPase from budding yeast. *Proc. Natl. Acad. Sci. USA* **106**, 16586-16591
 11. Coleman, J., Kwok, M., and Molday, R. (2009) Localization, purification, and functional reconstitution of the P₄-ATPase Atp8a2, a phosphatidylserine flippase in photoreceptor disc membranes. *J. Biol. Chem.* **284**, 32670-32679
 12. Misu, K., Fujimura-Kamada, K., Ueda, T., Nakano, A., Katoh, H., and Tanaka, K. (2003) Cdc50p, a conserved endosomal membrane protein, controls polarized growth in *Saccharomyces cerevisiae*. *Mol. Biol. Cell* **14**, 730-747
 13. Radji, M., Kim, J. M., Togan, T., Yoshikawa, H., and Shirahige, K. (2001) The cloning and characterization of the *CDC50* gene family in *Saccharomyces cerevisiae*. *Yeast* **18**, 195-205
 14. Kato, U., Emoto, K., Fredriksson, C., Nakamura, H., Ohta, A., Kobayashi, T.,

- Murakami-Murofushi, K., Kobayashi, T., and Umeda, M. (2002) A novel membrane protein, Ros3p, is required for phospholipid translocation across the plasma membrane in *Saccharomyces cerevisiae*. *J. Biol. Chem.* **277**, 37855-37862
15. Hanson, P., Malone, L., Birchmore, J., and Nichols, J. (2003) Lem3p is essential for the uptake and potency of alkylphosphocholine drugs, edelfosine and miltefosine. *J. Biol. Chem.* **278**, 36041-36050
16. Furuta, N., Fujimura-Kamada, K., Saito, K., Yamamoto, T., and Tanaka, K. (2007) Endocytic recycling in yeast is regulated by putative phospholipid translocases and the ypt31p/32p-rcy1p pathway. *Mol. Biol. Cell* **18**, 295-312
17. Chen, S., Wang, J., Muthusamy, B.P., Liu, K., Zare, S., Andersen, R.J., and Graham, T.R. (2006) Roles for the Drs2p-Cdc50p complex in protein transport and phosphatidylserine asymmetry of the yeast plasma membrane. *Traffic* **7**, 1503-1517
18. Paulusma, C.C., Folmer, D.E., Ho-Mok, K.S., de Waart, D.R., Hilarius, P.M., Verhoeven, A.J., and Oude Elferink, R.P. (2008) ATP8B1 requires an accessory protein for endoplasmic reticulum exit and plasma membrane lipid flippase activity. *Hepatology* **47**, 268-278
19. Poulsen, L., López-Marqués, R., McDowell, S., Okkeri, J., Licht, D., Schulz, A., Pomorski, T., Harper, J., and Palmgren, M. (2008) The *Arabidopsis* P₄-ATPase ALA3 localizes to the golgi and requires a β -subunit to function in lipid translocation and secretory vesicle formation. *Plant Cell* **20**, 658-676
20. López-Marqués, R., Poulsen, L., Hanisch, S., Meffert, K., Buch-Pedersen, M., Jakobsen, M.,

- Pomorski, T., and Palmgren, M. (2010) Intracellular targeting signals and lipid specificity determinants of the ALA/ALIS P₄-ATPase complex reside in the catalytic ALA α -subunit. *Mol. Biol. Cell* **21**, 791-801
21. Perez-Victoria, F.J., Sanchez-Canete, M.P., Castanys, S., and Gamarro, F. (2006) Phospholipid translocation and miltefosine potency require both *L. donovani* miltefosine transporter and the new protein LdRos3 in *Leishmania* parasites. *J. Biol. Chem.* **281**, 23766-23775
22. Lenoir, G., Williamson, P., Puts, C.F., and Holthuis, J.C. (2009) Cdc50p plays a vital role in the ATPase reaction cycle of the putative aminophospholipid transporter Drs2p. *J. Biol. Chem.* **284**, 17956-17967
23. Rose, M.D., Winston, F., and Hieter, P. (1990) *Methods in Yeast Genetics A Laboratory Course Manual*, Cold Spring Harbor Press, Cold Spring Harbor, NY.
24. Guthrie, C., and Fink, G.R. (1991) *Guide to Yeast Genetics and Molecular Biology*, Academic Press, San Diego, CA.
25. Elble, R. (1992) A simple and efficient procedure for transformation of yeasts. *Biotechniques* **13**, 18-20
26. Gietz, R.D., and Woods, R.A. (2002) Transformation of yeast by lithium acetate/single-stranded carrier DNA/polyethylene glycol method. *Methods Enzymol.* **350**, 87-96
27. Longtine, M.S., McKenzie, A., 3rd, Demarini, D.J., Shah, N.G., Wach, A., Brachat, A.,

- Philippsen, P., and Pringle, J.R. (1998) Additional modules for versatile and economical PCR-based gene deletion and modification in *Saccharomyces cerevisiae*. *Yeast* **14**, 953-961
28. Tong, A.H., Evangelista, M., Parsons, A.B., Xu, H., Bader, G.D., Page, N., Robinson, M., Raghizadeh, S., Hogue, C.W., Bussey, H., Andrews, B., Tyers, M., and Boone, C. (2001) Systematic genetic analysis with ordered arrays of yeast deletion mutants. *Science* **294**, 2364-2368
29. Cadwell, R.C., and Joyce, G.F. (1992) Randomization of genes by PCR mutagenesis. *PCR Methods Appl.* **2**, 28-33
30. Toi, H., Fujimura-Kamada, K., Irie, K., Takai, Y., Todo, S., and Tanaka, K. (2003) She4p/Dim1p interacts with the motor domain of unconventional myosins in the budding yeast, *Saccharomyces cerevisiae*. *Mol. Biol. Cell* **14**, 2237-2249
31. Franzusoff, A., Redding, K., Crosby, J., Fuller, R.S., and Schekman, R. (1991) Localization of components involved in protein transport and processing through the yeast Golgi apparatus. *J. Cell Biol.* **112**, 27-37
32. Chuang, J.S., and Schekman, R.W. (1996) Differential trafficking and timed localization of two chitin synthase proteins, Chs2p and Chs3p. *J. Cell Biol.* **135**, 597-610
33. Ziman, M., Chuang, J.S., Tsung, M., Hamamoto, S., and Schekman, R. (1998) Chs6p-dependent anterograde transport of Chs3p from the chitosome to the plasma membrane in *Saccharomyces cerevisiae*. *Mol. Biol. Cell* **9**, 1565-1576
34. Valdivia, R., Baggott, D., Chuang, J., and Schekman, R. (2002) The yeast clathrin adaptor

protein complex 1 is required for the efficient retention of a subset of late Golgi membrane proteins. *Dev. Cell* **2**, 283-294

35. Liu, K., Surendhran, K., Nothwehr, S., and Graham, T.R. (2008) P4-ATPase requirement for AP-1/clathrin function in protein transport from the *trans*-Golgi network and early endosomes. *Mol. Biol. Cell* **19**, 3526-3535
36. Lewis, M.J., Nichols, B.J., Prescianotto-Baschong, C., Riezman, H., and Pelham, H.R. (2000) Specific retrieval of the exocytic SNARE Snc1p from early yeast endosomes. *Mol. Biol. Cell* **11**, 23-38
37. Geering, K. (2001) The functional role of β subunits in oligomeric P-type ATPases. *J. Bioenerg. Biomembr.* **33**, 425-438
38. Sikorski, R.S., and Hieter, P. (1989) A system of shuttle vectors and yeast host strains designed for efficient manipulation of DNA in *Saccharomyces cerevisiae*. *Genetics* **122**, 19-27
39. Gietz, R.D., and Sugino, A. (1988) New yeast-*Escherichia coli* shuttle vectors constructed with in vitro mutagenized yeast genes lacking six-base pair restriction sites. *Gene* **74**, 527-534

Figure legends

Fig. 1. The growth defect and localization of Cdc50p-ts-EGFP in newly isolated *cdc50-ts*

mutants. (A) The temperature-sensitive growth of *cdc50-ts* mutants. The *cdc50Δ lem3Δ crf1Δ* cells harboring plasmids containing the indicated alleles of *cdc50-EGFP* were streaked on YPDA plates and grown at 25°C or 37°C for 2 d. The yeast strains used were: YKT1190 (*CDC50-EGFP*); YKT1247 (*cdc50-ts1-10-EGFP*); YKT1248 (*cdc50-ts3-7-EGFP*); YKT1249 (*cdc50-ts4-7-EGFP*); YKT1250 (*cdc50-ts7-27-EGFP*); YKT1251 (*cdc50-ts8-10-EGFP*); YKT1252 (*cdc50-ts9-4-EGFP*). (B) Localization of Cdc50p-ts-EGFP at 37°C. The *cdc50-ts* mutants described in (A) were grown to early logarithmic phase in SD-Leu medium at 25°C, and shifted to 37°C for 2 h, followed by microscopic observation. Bar, 5 μm. (C) Colocalization of Cdc50p-ts-EGFP with Sec7p-mRFP1. The *cdc50Δ sec7-mRFP1* strains harboring *cdc50-ts* plasmids were grown as in (B) and microscopically observed except that cells were fixed in 0.5% formaldehyde before observation. Obtained images were merged to demonstrate the coincidence of the two signal patterns. The Cdc50p-EGFP dots were examined for colocalization with Sec7p-mRFP1 by observing more than 300 Cdc50p-EGFP dots (> 100 cells) for each strain. The colocalization efficiency is shown in the lower panel in comparison with that at 25°C. The yeast strains used were: YKT1240 (*CDC50-EGFP*); YKT1241 (*cdc50-ts1-10-EGFP*); YKT1242 (*cdc50-ts3-7-EGFP*); YKT1243 (*cdc50-ts4-7-EGFP*); YKT1244 (*cdc50-ts7-27-EGFP*); YKT1245 (*cdc50-ts8-10-EGFP*); YKT1246 (*cdc50-ts9-4-EGFP*). Bar, 5 μm.

Fig. 2. Amino acid substitutions in the Cdc50-ts proteins. (A) The domain structure of Cdc50p and the amino-acid substitutions in the Cdc50p-ts proteins. Mutants with single substitution are indicated with rectangles, whereas those with more than two are indicated with rounded-rectangles. Two gray boxes (TM) indicate the potential transmembrane domains. The *NheI* restriction enzyme site is shown underneath. (B) Alignment of Cdc50 family proteins and the amino-acid substitutions. Full-length amino acid sequences were initially aligned using the clustal W program (<http://clustalw.ddbj.nig.ac.jp/top-j.html>) and then shaded according to BOXSHADE (http://www.ch.embnet.org/software/BOX_form.html). Only the region around the mutation sites is shown. The bars indicate the potential transmembrane domains. The GenBank accession numbers are: CDC50 (NP_010018), LEM3 (NP_014076), CRF1 (NP_014446), fission-yeast (NP_595126), Candida (XP_718073), nematode (NP_001023332), fruit fly (NP_573128), Arabidopsis (NP_566435), zebrafish (NP_991123), mouse (NP_848830), and human (NP_001017970) (C) Growth curves of *cdc50-ts* mutants. Wild-type and the *cdc50-ts* mutants were grown to early logarithmic phase in YPDA medium at 25°C, shifted to 37°C at 0 h, and cell numbers were counted at the indicated time point. The strains used are the same as in Fig. 1A.

Fig. 3. Cdc50p-ts7-27-EGFP and Cdc50p-ts9-4-EGFP form a complex with Drs2p. (A)

Colocalization of Cdc50p-ts7-27-EGFP and Cdc50p-ts9-4-EGFP with Drs2p-mRFP1.

cdc50Δ lem3Δ crf1Δ DRS2-mRFP1 cells harboring the *CDC50-EGFP*, *cdc50-ts7-27-EGFP*, or

cdc50-ts9-4-EGFP plasmid were grown to early logarithmic phase in SD-Leu medium at 25°C and shifted to 37°C for 2 h. Images were merged to demonstrate the coincidence of signal patterns. An arrow in *cdc50-ts9-4* indicates the Drs2p-mRFP signal showing the ER-like pattern. The yeast strains used were: YKT1253 (*CDC50-EGFP*); YKT1257 (*cdc50-ts7-27-EGFP*); YKT1259 (*cdc50-ts9-4-EGFP*). Bar, 5 μm. (B) Co-immunoprecipitation of Cdc50p-ts7-27-EGFP and Cdc50p-ts9-4-EGFP with Drs2p-13Myc. Cells were grown at 25°C and shifted to 37°C for 2 h to a cell density of 0.8 OD₆₀₀/ml in SD-Leu medium. Membrane extracts were prepared as described in Materials and Methods. Myc-tagged Drs2p was immunoprecipitated with an anti-Myc antibody from membrane extracts. Immunoprecipitates were subjected to SDS-PAGE, followed by immunoblot analysis using antibodies against Myc and Cdc50p. The results shown are representatives of several experiments. The band intensity was quantitated by an image analyzing system, and the relative percentages of mutant Cdc50p-EGFP bound to Drs2-13Myc were calculated. The values represent averages of three independent experiments with the standard deviations. The yeast strains used were: YKT1260 (*DRS2-13Myc CDC50-EGFP*); YKT1190 (*DRS2 CDC50-EGFP*); YKT1264 (*DRS2-13Myc cdc50-ts7-27-EGFP*); YKT1266 (*DRS2-13Myc cdc50-ts9-4-EGFP*).

Fig. 4. The *cdc50-ts7-27* and *cdc50-ts9-4* mutations restored CW sensitivity to *chs6Δ* cells.

Five-fold serial dilutions of cells starting with a suspension at 5 x 10⁶ cells/ml in YPDA were spotted in 4-μl drops onto YPDA plates (left) or YPDA containing 0.1 mg/ml CW plates (right).

The plates were incubated at 30°C or 37°C for 35 h. The yeast strains used were: YKT38 (wild-type); YKT1655 (*chs6Δ*); YKK1183 (*chs6Δ cdc50Δ* [pRS315 (vector)]); YKK1177 (*chs6Δ cdc50Δ* [pRS315-*CDC50-EGFP*]); YKK1179 (*chs6Δ cdc50Δ* [pRS315-*cdc50-ts7-27-EGFP*]); YKK1181 (*chs6Δ cdc50Δ* [pRS315-*cdc50-ts9-4-EGFP*]); YKT1705 (*chs6Δ apl2Δ*).

Fig. 5. The *cdc50-ts7-27* and *cdc50-ts9-4* mutants exhibit defects in endocytic recycling and mutant Cdc50 proteins and Drs2p accumulate in early endosome-derived structures. (A)

Colocalization of Cdc50p-ts-EGFP and mRFP1-Snc1p. *cdc50Δ lem3Δ crf1Δ mRFP1-SNC1* cells harboring the *CDC50-EGFP*, *cdc50-ts7-27-EGFP*, or *cdc50-ts9-4-EGFP* gene on a centromeric plasmid were grown to early logarithmic phase in SD-Leu medium at 25°C, and shifted to 37°C for 2 h. Images were merged to compare the two signal patterns. The yeast strains used were:

YKT1372 (*CDC50-EGFP*); YKT1373 (*cdc50-ts7-27-EGFP*); YKT1374 (*cdc50-ts9-4-EGFP*). (B)

Colocalization of Drs2p-EGFP and mRFP1-Snc1p. *cdc50Δ lem3Δ crf1Δ DRS2-EGFP mRFP1-SNC1* cells harboring the *CDC50*, *cdc50-ts7-27*, or *cdc50-ts9-4* gene on a centromeric plasmid were grown and analyzed as in (A). The yeast strains used were: YKT1706 (*CDC50*); YKT1707 (*cdc50-ts7-27*); YKT1708 (*cdc50-ts9-4*). Bars, 5 μm.

Table 1

***Saccharomyces cerevisiae* strains used in this study.**

Strain ^a	Genotype	Reference or source
YEF473	<i>MATa</i> α <i>his3</i> Δ -200/ <i>his3</i> Δ -200 <i>leu2</i> Δ -1/ <i>leu2</i> Δ -1 <i>lys2</i> -801/ <i>lys2</i> -801 <i>ura3</i> -52/ <i>ura3</i> -52 <i>trp1</i> Δ -63/ <i>trp1</i> Δ -63	(27)
YKT38	<i>MATa</i> <i>his3</i> Δ -200 <i>leu2</i> Δ -1 <i>lys2</i> -801 <i>ura3</i> -52 <i>trp1</i> Δ -63	(12)
YKT902	<i>MATa</i> <i>lem3</i> Δ :: <i>TRP1</i> <i>crf1</i> Δ :: <i>hphMX3</i>	(16)
YKT1142	<i>MAT</i> α <i>cdc50</i> Δ :: <i>HIS3MX6</i> <i>lem3</i> Δ :: <i>TRP1</i> <i>crf1</i> Δ :: <i>hphMX3</i> [<i>YCplac33-CDC50 URA3</i>]	This study
YKT1149	<i>MATa</i> <i>cdc50</i> Δ :: <i>HIS3MX6</i> <i>SEC7-mRFP1</i> :: <i>TRP1</i>	This study
YKT1190	<i>MAT</i> α <i>cdc50</i> Δ :: <i>HIS3MX6</i> <i>lem3</i> Δ :: <i>TRP1</i> <i>crf1</i> Δ :: <i>hphMX3</i> [<i>pRS315-CDC50-EGFP</i>]	This study
YKT1240	<i>MATa</i> <i>cdc50</i> Δ :: <i>HIS3MX6</i> <i>SEC7-mRFP1</i> :: <i>TRP1</i> [<i>pRS315-CDC50-EGFP</i>]	This study
YKT1241	<i>MATa</i> <i>cdc50</i> Δ :: <i>HIS3MX6</i> <i>SEC7-mRFP1</i> :: <i>TRP1</i> [<i>pRS315-cdc50-ts1-10-EGFP</i>]	This study
YKT1242	<i>MATa</i> <i>cdc50</i> Δ :: <i>HIS3MX6</i> <i>SEC7-mRFP1</i> :: <i>TRP1</i> [<i>pRS315-cdc50-ts3-7-EGFP</i>]	This study
YKT1243	<i>MATa</i> <i>cdc50</i> Δ :: <i>HIS3MX6</i> <i>SEC7-mRFP1</i> :: <i>TRP1</i> [<i>pRS315-cdc50-ts4-7-EGFP</i>]	This study

YKT1244	<i>MATa cdc50Δ::HIS3MX6 SEC7-mRFP1::TRP1</i> <i>[pRS315-cdc50-ts7-27-EGFP]</i>	This study
YKT1245	<i>MATa cdc50Δ::HIS3MX6 SEC7-mRFP1::TRP1</i> <i>[pRS315-cdc50-ts8-10-EGFP]</i>	This study
YKT1246	<i>MATa cdc50Δ::HIS3MX6 SEC7-mRFP1::TRP1</i> <i>[pRS315-cdc50-ts9-4-EGFP]</i>	This study
YKT1247	<i>MATα cdc50Δ::HIS3MX6 lem3Δ::TRP1 crf1Δ::hphMX3</i> <i>[pRS315-cdc50-ts1-10-EGFP]</i>	This study
YKT1248	<i>MATα cdc50Δ::HIS3MX6 lem3Δ::TRP1 crf1Δ::hphMX3</i> <i>[pRS315-cdc50-ts3-7-EGFP]</i>	This study
YKT1249	<i>MATα cdc50Δ::HIS3MX6 lem3Δ::TRP1 crf1Δ::hphMX3</i> <i>[pRS315-cdc50-ts4-7-EGFP]</i>	This study
YKT1250	<i>MATα cdc50Δ::HIS3MX6 lem3Δ::TRP1 crf1Δ::hphMX3</i> <i>[pRS315-cdc50-ts7-27-EGFP]</i>	This study
YKT1251	<i>MATα cdc50Δ::HIS3MX6 lem3Δ::TRP1 crf1Δ::hphMX3</i> <i>[pRS315-cdc50-ts8-10-EGFP]</i>	This study
YKT1252	<i>MATα cdc50Δ::HIS3MX6 lem3Δ::TRP1 crf1Δ::hphMX3</i> <i>[pRS315-cdc50-ts9-4-EGFP]</i>	This study
YKT1253	<i>MATα cdc50Δ::HIS3MX6 lem3Δ::kanMX4 crf1Δ::hphMX3</i> <i>DRS2-mRFP1::TRP1 [pRS315-CDC50-EGFP]</i>	This study

YKT1257	<i>MATα cdc50Δ::HIS3MX6 lem3Δ::kanMX4 crf1Δ::hphMX3</i> <i>DRS2-mRFP1::TRP1 [pRS315-cdc50-ts7-27-EGFP]</i>	This study
YKT1259	<i>MATα cdc50Δ::HIS3MX6 lem3Δ::kanMX4 crf1Δ::hphMX3</i> <i>DRS2-mRFP1::TRP1 [pRS315-cdc50-ts9-4-EGFP]</i>	This study
YKT1260	<i>MATα cdc50Δ::HIS3MX6 lem3Δ::kanMX4 crf1Δ::hphMX3</i> <i>DRS2-13Myc::TRP1 [pRS315-CDC50-EGFP]</i>	This study
YKT1264	<i>MATα cdc50Δ::HIS3MX6 lem3Δ::kanMX4 crf1Δ::hphMX3</i> <i>DRS2-13Myc::TRP1 [pRS315-cdc50-ts7-27-EGFP]</i>	This study
YKT1266	<i>MATα cdc50Δ::HIS3MX6 lem3Δ::kanMX4 crf1Δ::hphMX3</i> <i>DRS2-13Myc::TRP1 [pRS315-cdc50-ts9-4-EGFP]</i>	This study
YKT1371	<i>MATα lem3Δ::TRP1 crf1Δ::hphMX3 URA3::mRFP-SNC1</i>	This study
YKT1372	<i>MATα cdc50Δ::HIS3MX6 lem3Δ::TRP1 crf1Δ::hphMX3</i> <i>URA3::mRFP1-SNC1 [pRS315-CDC50-EGFP]</i>	This study
YKT1373	<i>MATα cdc50Δ::HIS3MX6 lem3Δ::TRP1 crf1Δ::hphMX3</i> <i>URA3::mRFP1-SNC1 [pRS315-cdc50-ts7-27-EGFP]</i>	This study
YKT1374	<i>MATα cdc50Δ::HIS3MX6 lem3Δ::TRP1 crf1Δ::hphMX3</i> <i>URA3::mRFP1-SNC1 [pRS315-cdc50-ts9-4-EGFP]</i>	This study
YKT1655	<i>MATα chs6Δ::kanMX4</i>	This study
YKT1697	<i>MATα cdc50Δ::TRP1</i>	This study

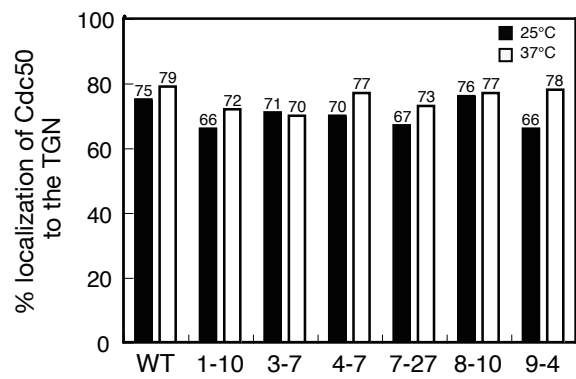
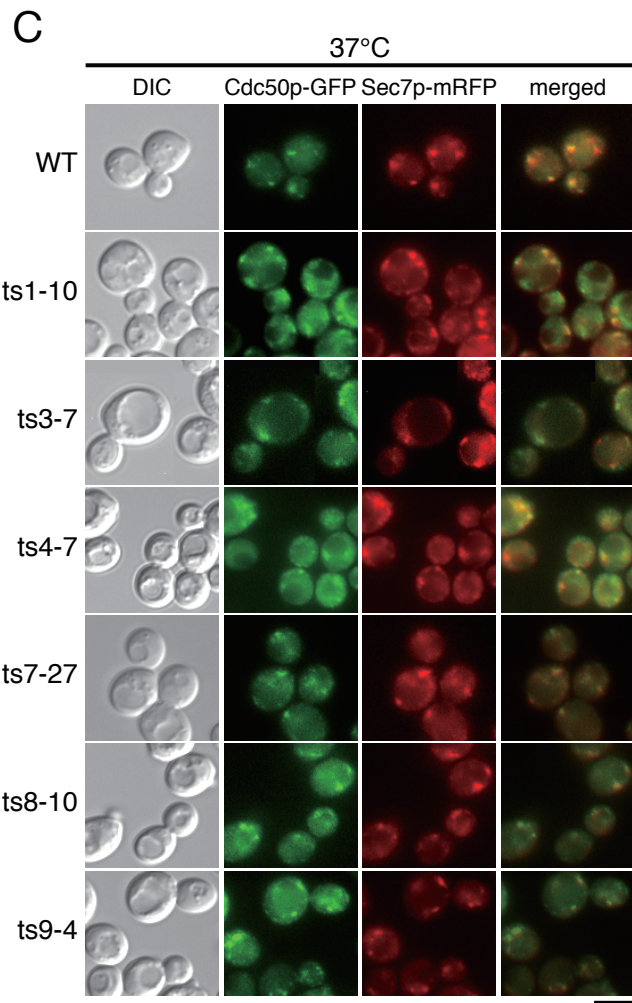
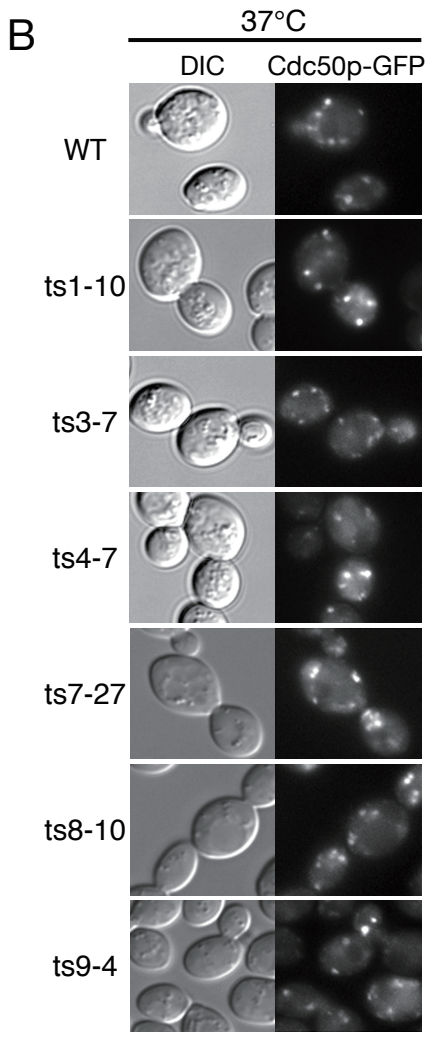
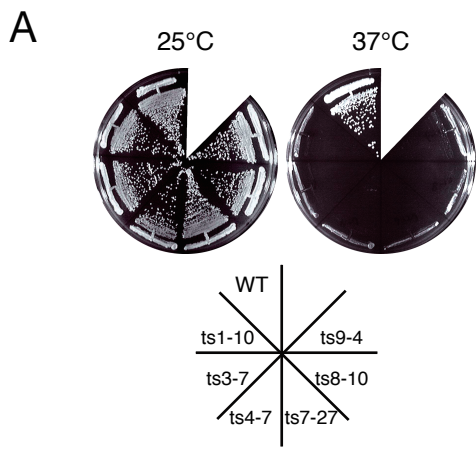
YKT1701	<i>MATa chs6Δ::kanMX4 cdc50Δ::HIS3MX6</i>	This study
YKT1705	<i>MATa chs6Δ::kanMX4 apl2Δ::hphMX4</i>	This study
YKT1706	<i>MATa cdc50Δ::HIS3MX6 lem3Δ::TRP1 crf1Δ::hphMX3</i> <i>DRS2-EGFP::kanMX6 URA3::mRFP1-SNC1 [pRS315-CDC50]</i>	This study
YKT1707	<i>MATa cdc50Δ::HIS3MX6 lem3Δ::TRP1 crf1Δ::hphMX3</i> <i>DRS2-EGFP::kanMX6 URA3::mRFP1-SNC1</i> <i>[pRS315-cdc50-ts7-27]</i>	This study
YKT1708	<i>MATa cdc50Δ::HIS3MX6 lem3Δ::TRP1 crf1Δ::hphMX3</i> <i>DRS2-EGFP::kanMX6 URA3::mRFP1-SNC1</i> <i>[pRS315-cdc50-ts9-4]</i>	This study
YKK1177	<i>MATa chs6Δ::kanMX4 cdc50Δ::HIS3MX6</i> <i>[pRS315-CDC50-EGFP]</i>	This study
YKK1179	<i>MATa chs6Δ::kanMX4 cdc50Δ::HIS3MX6</i> <i>[pRS315-cdc50-ts7-27-EGFP]</i>	This study
YKK1181	<i>MATa chs6Δ::kanMX4 cdc50Δ::HIS3MX6</i> <i>[pRS315-cdc50-ts9-4-EGFP]</i>	This study
YKK1183	<i>MATa chs6Δ::kanMX4 cdc50Δ::HIS3MX6 [pRS315]</i>	This study

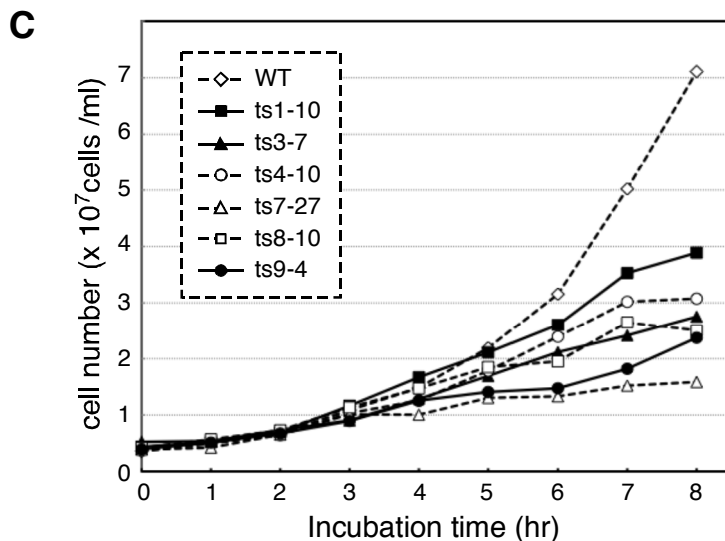
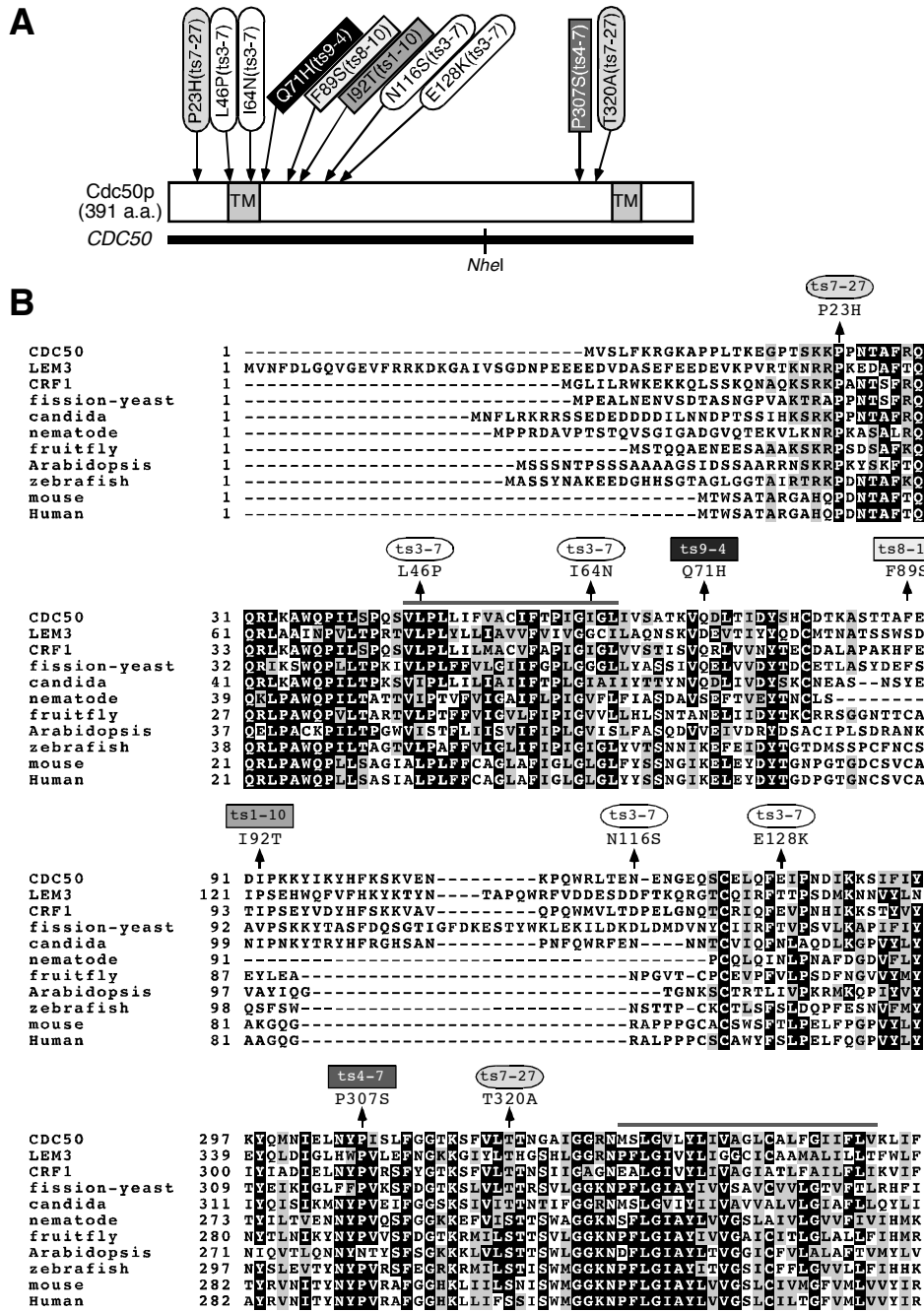
a YKT and YKK strains are isogenic derivatives of YEF473. For YKT and YKK strains, only relevant genotypes are described.

Table 2**Plasmids used in this study.**

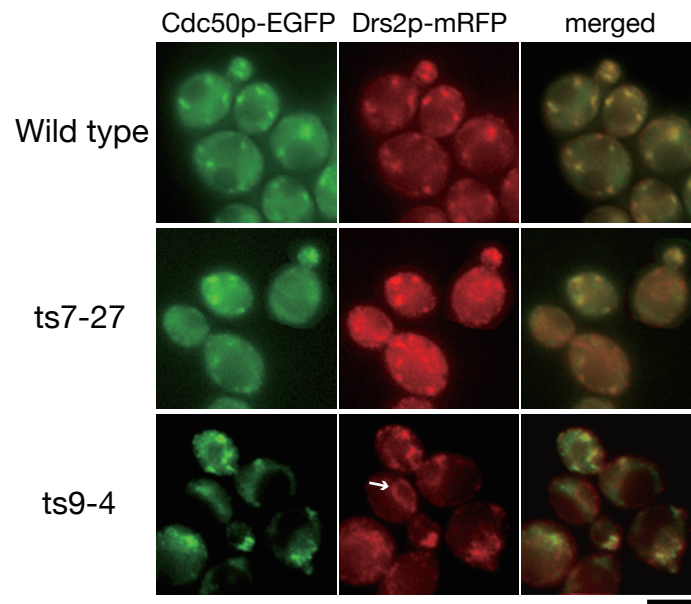
Plasmid	Characteristics	Reference or source
pKT1261 [YCplac33-CDC50]	<i>CDC50 URA3 CEN</i>	This study
pKT1466 [pRS315-CDC50-EGFP]	<i>CDC50-EGFP LEU2 CEN</i>	This study
pKT1589 [pRS315-cdc50-ts1-10-EGFP]	<i>cdc50-ts1-10-EGFP LEU2 CEN</i>	This study
pKT1590 [pRS315-cdc50-ts3-7-EGFP]	<i>cdc50-ts3-7-EGFP LEU2 CEN</i>	This study
pKT1591 [pRS315-cdc50-ts4-7-EGFP]	<i>cdc50-ts4-7-EGFP LEU2 CEN</i>	This study
pKT1592 [pRS315-cdc50-ts7-27-EGFP]	<i>cdc50-ts7-27-EGFP LEU2 CEN</i>	This study
pKT1593 [pRS315-cdc50-ts8-10-EGFP]	<i>cdc50-ts8-10-EGFP F89S LEU</i>	This study
pKT1594 [pRS315-cdc50-ts9-4-EGFP]	<i>cdc50-ts9-4-EGFP LEU2 CEN</i>	This study
pKT1598 [pRS315-cdc50-ts7-27]	<i>cdc50-ts7-27 LEU2 CEN</i>	This study
pKT1600 [pRS315-cdc50-ts9-4]	<i>cdc50-ts9-4 LEU2 CEN</i>	This study
pKT1601 [pRS315-CDC50]	<i>CDC50 LEU2 CEN</i>	This study
pKT1654 [pRS306-mRFP1-SNC1]	<i>P_{TPH}-mRFP1-SNC1 URA3</i>	This study
pKT1829	<i>CDC50-EGFP-HIS3MX6</i>	This study
[pUC119-CDC50-EGFP-HIS3MX6]		
pKT1830	<i>cdc50-ts7-27-EGFP-HIS3MX6</i>	This study
[pUC119-cdc50-ts7-27-EGFP-HIS3MX6]		

pKT1831	<i>cdc50-ts9-4-EGFP-HIS3MX6</i>	This study
[pUC119- <i>cdc50-ts9-4-EGFP-HIS3MX6</i>]		
pRS315	<i>LEU2 CEN</i>	(38)
pRS306	<i>URA3</i>	(38)
YCplac33	<i>URA3 CEN</i>	(39)





A



B

